Original Research Article

Nonlinear finite element analysis for Concrete Deep Beam Reinforced with GFRP Bars

ABSTRACT

Deep concrete beams with small shear span-depth ratios (a/d) are common structural elements. Members internally reinforced with fiber-reinforced polymer (FRP) are increasingly specified to prevent corrosion-induced damage in concrete constructions. Until now, the majority of studies have concentrated on the behavior of shallow beams longitudinally reinforced with (GFRP), and most of them have used small-scale testing. The flexural performance of concrete deep beam reinforced with locally manufactured (GFRP) bars was investigated using one half-scale concrete deep beam, the beam tested under one-point bending configuration. ANSYS Software was used to perform nonlinear finite element analysis NLFEA which used to compare with the test results. Also, parametric studies have been performed to examine the influence of (GFRP) reinforcement ratio. The validity of the program was confirmed by comparing it to accessible experimental data, and the agreement was found to be satisfactory. A parametric analysis was also carried out to see how the ratio of (GFRP) bars affects the behavior of deep beams.

KEYWORDS: DEEP BEAMS; GFRB; FINITE ELEMENT.

1. INTRODUCTION

In the civil and structural engineering sectors, composite materials, such as Fiber Reinforced Polymer (FRP) bars, have been gaining traction as alternatives to traditional steel reinforcements (FRP) materials are non-corrosive, making them an excellent substitute for steel reinforcement in harsh conditions. They are also lightweight and have a high longitudinal tensile strength. [1]. In the construction business, the long-term durability of reinforced concrete constructions has become a major concern. One of the leading reasons of reinforced concrete structure service life reduction is the rapid corrosion of steel reinforcement bars. Dams, tanks, and bridges, for example, were exposed to moisture,

chlorides, and de-icing salts, causing steel reinforcing to corrode. Steel reinforcing bars should be changed or coated with non-corrosive materials to solve this problem and meet the requirements for ultimate limit state and durability for these buildings. Fiber reinforced polymer (FRP) bars have recently been employed as an alternative material to steel reinforcement bars that have corroded. Carbon (CFRP), glass (GFRP), and aramid fibers are the most popular forms of fibers (AFRP). FRP bars have a good corrosion resistance and a high specific strength. Corrosion of steel reinforcement in concrete constructions causes concrete to crack and spall, requiring expensive maintenance and repair. As a result, by replacing the steel reinforcement with non-corrosive (FRP) reinforcement, the possibility of corrosion and subsequent deterioration is eliminated [2]. Many steel-reinforced concrete structures, such as bridges, parking garages, and offshore vessels, are subjected to harsh environments that, over time, can cause substantial damage and necessitate costly rehabilitation due to steel reinforcement corrosion. The flexural and shear behavior of slender (shallow) concrete elements reinforced with (FRP) reinforcement has been the subject of extensive research [3]. A deep beam is a member with a small shear span-to-depth (a/d) ratio [4]. In another words, a beam with a (a/d) ratio of less than 4 can be considered a deep beam [5]. Matthias et al. [3] presented a twelve-large-scale beam experimental examination. The specimens' height, shear span-to-depth (a/d) ratio, reinforcing ratio (ρ), and concrete compressive strength (fc) were the main factors. To investigate the concrete contribution to shear capacity, no distributed or transverse web reinforcing was incorporated in the tested specimens. Longitudinal reinforcement was provided by the (GFRP) bars. When the reinforcement ratio was raised, the normalized shear capacity increased by 3%. Reduced normalized shear stress at the ultimate load is a result of increased member height. By increasing concrete strength, the normalized shear capacity decreases. Ahmed et al. [6] studied the shear behavior of four full-scale deep beams reinforced with carbon fiber reinforced plastic (CFRP) and glass fiber reinforced plastic (GFRP) bars. The key test factors were the longitudinal reinforcement ratio and the type of reinforcement. The ultimate capacity and deflection were significantly affected by the reinforcement ratio and concrete compressive strength, whereas the reinforcement type had no discernible effect on the behavior of the tested beams. All of the test beams failed due to brittle failure.

2. Experimental program

2.1. Test specimen

As a simply supported span, one half-scale reinforced concrete deep beam with a reasonable amount of longitudinal and shear reinforcement was designed. The specimen was reinforced with 2ϕ16 (GFRP) bars as tension reinforcement. The 16 mm diameter (GFRP) bars had an ultimate strength of around 850 MPa. In addition, the concrete's cubic compressive strength (fcu) was 25 MPa. This study looked into the effects of using (GFRP) bars as reinforcement bars on the behavior of reinforced concrete deep beams. The mean stress-strain curve for (GFRP) bars is shown in Figure. 1. The arrangement of the tested beam is shown in Figure. 2.

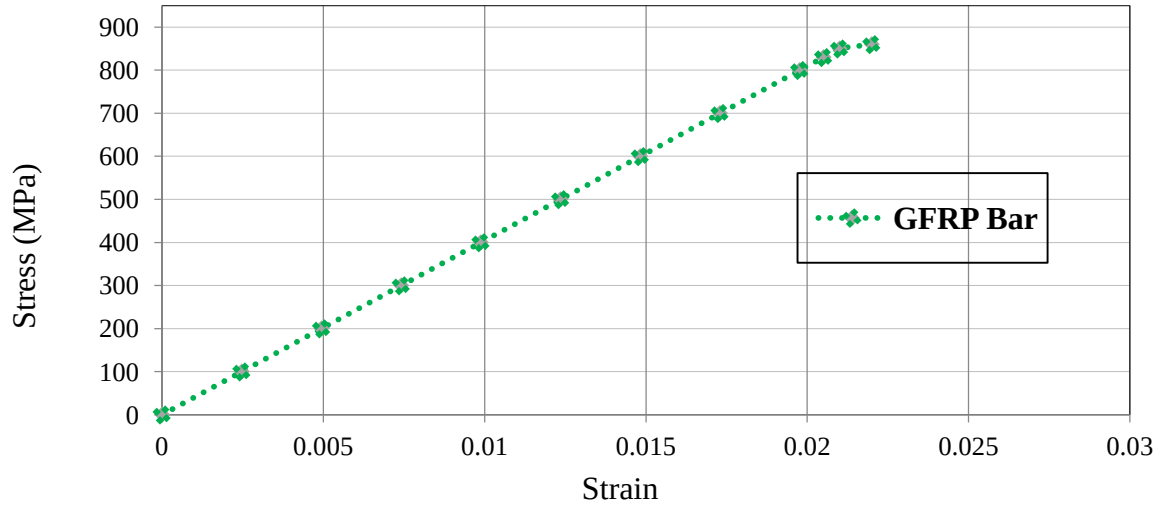

Figure.1 The mean stress-strain curve for (GFRP) bars.

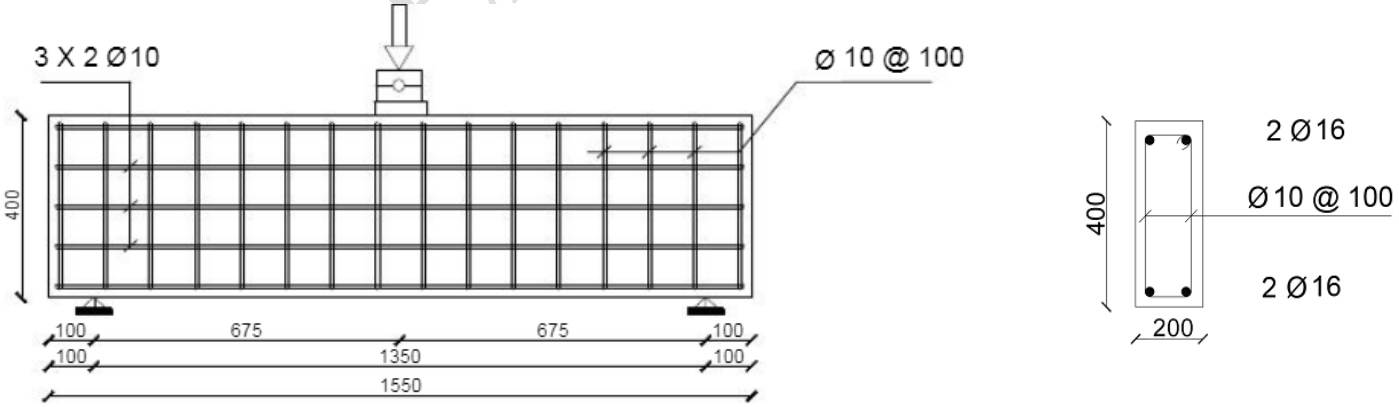

Figure 2 Tested Beams Geometry and Details.

2.3. Test setup

The specimen were placed through the test under load control. Strain gauges were placed at the longitudinal and shear reinforcement bars to measure the strain of the bars, as illustrated in Figure. 3. The deflection at the centerline was measured using a linear variable differential transformer (LVDT) positioned at the center span. The cracks were marked during the loading stages till the specimen failed. The (LVDT) installation is shown in Figure. 4. The deep beam was tested in a machine of 650 kN capacity. The load was concentrated on one plate. The loads was symmetrical to the centerline of the deep beam.

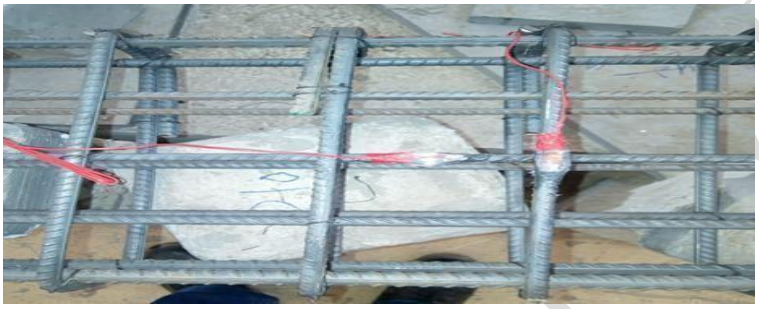

Figure 3. Installation of strain gauges.

Figure 4. LVDT installation.

3. Experimental results and discussion

3.1 Crack and ultimate load and Crack pattern

The deep beam was visually observed until the first crack appeared, with the corresponding first crack load being recorded. The initial crack in this beam occurred in the compression zone, and it was a shear inclined crack. The flexure cracks in the tension zone will have to appear quickly. As the load increases, the deflection of the beam increases rapidly. As the applied load increases, the primary shear crack linking the loading plate to the right side support will develop. Following that, the concrete under the loading plate will be crushed, resulting in a significant reduction in load-carrying capacity, as illustrated by the cracking pattern. At final level, the brittle failure happens suddenly and the mode of failure of this specimen was shear compression failure. The crack pattern for specimen B8 at failure is shown in Figure. 5.

Figure 5. Cracks pattern for specimen B8 at failure.

4. Non-Linear Finite Elements Analysis (NLFE)

To simulate the tested concrete deep beams, NLFEA was used. ANSYS (ANSYS release 15.1) [7], a commercially accessible finite element (FE) analysis software program, was used. The load–deflection curve is an important factor of beam behavior verification. It includes beneficial parameter which is the ratio of (GFRP) bars.

4.1Finite Element Formulation

To simulate the tested concrete deep beams, NLFEA was used. ANSYS (ANSYS release 15.1) [7], a commercially accessible finite element (FE) analysis software program, was used. The load–deflection curve is an important factor of beam behavior verification. It includes

beneficial parameter which is the ratio of (GFRP) bars. The 3-D model for a typical deep beam is presented in Figure.6.

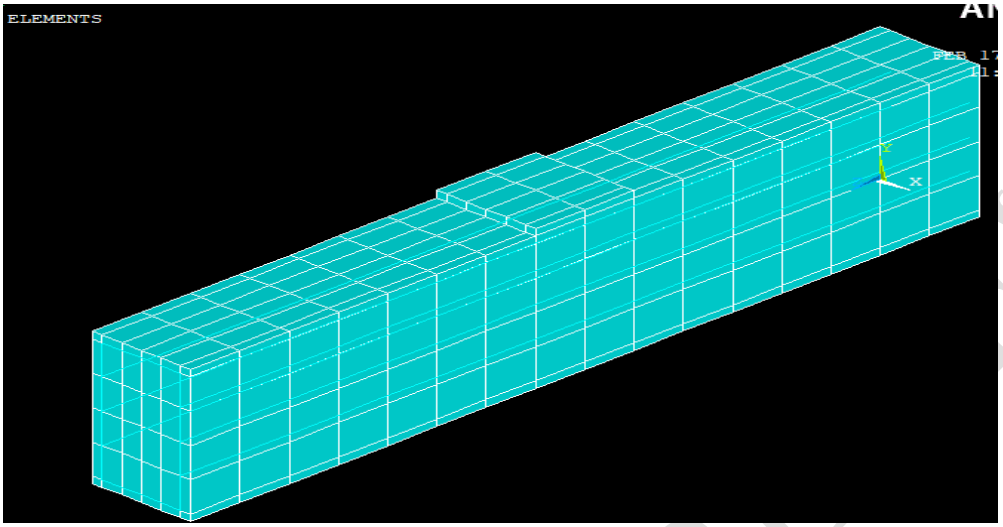

(a) Concrete Element; Solid65

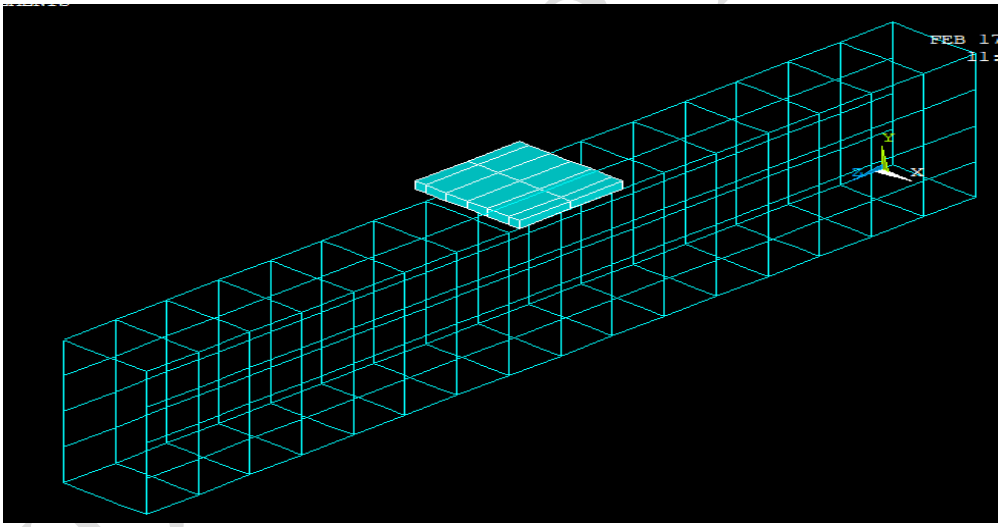

(b) Reinforcing Bar Element; Link8

Figure 6. Models for the Tested Deep Beams based on Finite Element Simulation.

Solid 65 for concrete is the structural element type utilized for geometric idealization of the diverse materials because of its ability to plastic deformation, cracking, and crushing in three directions. For idealized reinforcing bars and stirrups, 3-D spar elements (Link 8) were employed. It has two node and three DOF. It also has the ability to deform plastically. To avoid stress concentration problems. Five deep beam specimens (B1, B2, B3 and B4) of

rectangular shape with dimensions of 200 X 400 X 1550 mm. These specimens were reinforced with different reinforcement ratios of (GFRP) bars (0.15%, 0.41%, 0.53%, 0.67% and 0.79%). It should be mentioned that the deep beam specimen, B3 with 2ϕ16 (GFRP) bars was investigated experimentally. This specimen considered as a control specimen to verify the .analytical results

The Hognestad-Popvics stress–strain curve [8] was utilized for concrete in compression. A linear-tension curve was utilized for concrete in tension [9]. The bilinear stress–strain curve was employed for steel reinforcement in tension and compression [10], while the (GFRP) bars had a linear elastic behavior. The concrete and bars were thought to have a perfect connection.

4.2Analytical procedures

An incremental load approach was used to accommodate for non-linear analysis in the numerical solution scheme. The iterative solution used for each load increment was a blend of the traditional Newton-Raphson method's high convergence rate and the low cost of the modified Newton-Raphson approach, in which the stiffness was reformulated every loading step. Only transitory degrees of freedom were considered in the convergence criterion, which was based on iterative nodal displacement. The criterion is:

$$\psi / R \leq \phi$$

where ψ is the iterative displacement norm and R is the total displacement norm. The convergence tolerance, which ϕ was found to be between 0.01 and 0.05, produced satisfactory results. The analytical ultimate load of the test specimen has been defined as the load level at which the convergence criteria was not met, suggesting numerical instability.

4. Results of non-linear finite element analysis

4.1.Crack patterns

Figure. 7 shows the NLFEA outputs, which depict the crack propagation for Specimen B3 as an example. The first cracks occurred near the maximum tension zone in the mid-span, as illustrated in the crack formation diagram. As the load was increased, additional cracks appeared in the shear zone. As the load increases, the number of cracks increases as well. Following that, the cracks propagated upward through the depth of the beam, correlating with experiment results. Crack development and propagation patterns were comparable in all beams.

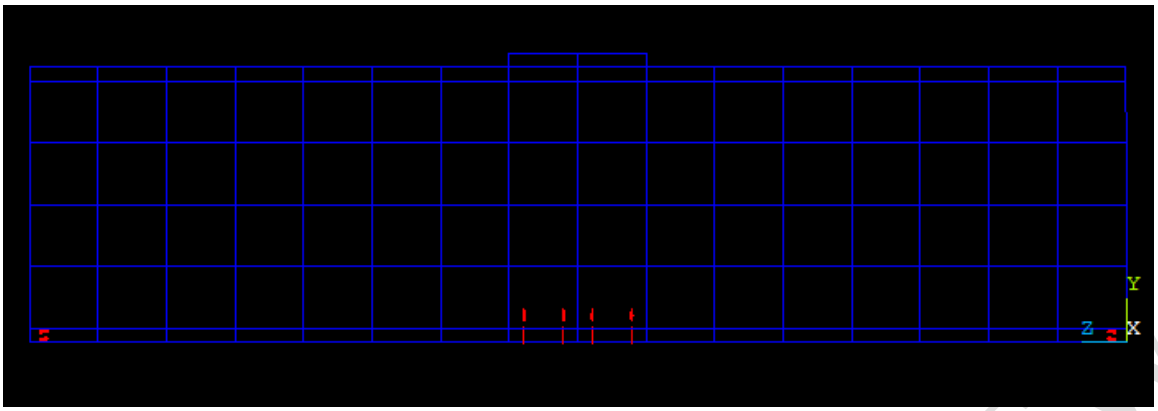

(a) At first load.

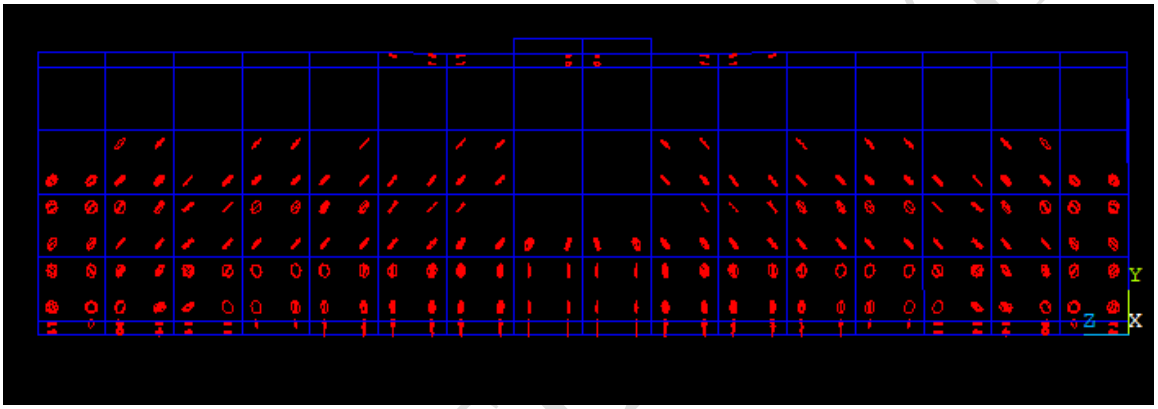

(b) At 50% of ultimate load.

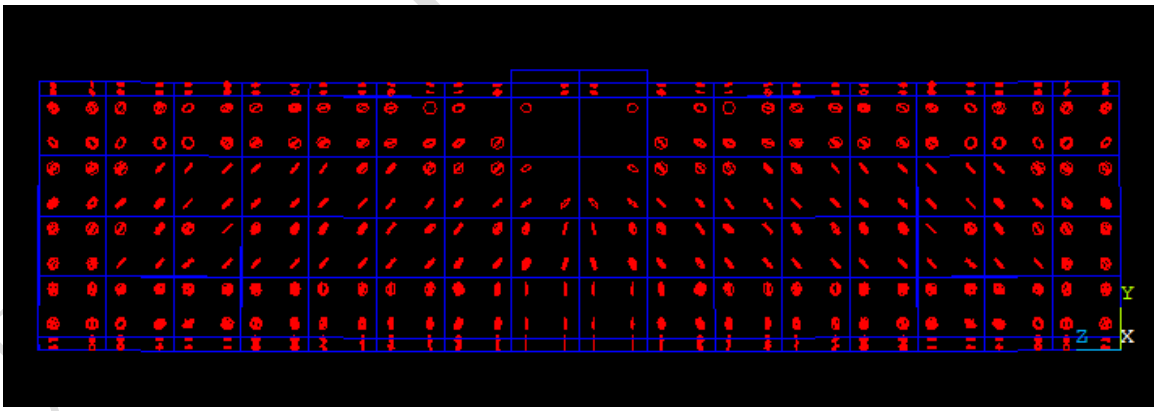

(c) At ultimate load.

Figure 7. Crack pattern for specimen B3.

4.2.Load-deflection behavior

According to Figure.8, for the majority of the test specimens, the NLFEA provided a fair estimate of the central deflection throughout the loading stages. Five specimens of deep beams reinforced with varied ratios of reinforcing bars were developed when it was discovered that the model achieved and confirmed the experimental test. According to Figure.9, increasing the reinforcement ratio leads to increase the ultimate load of tested beams. Furthermore, it was clear that the reinforcement ratio had an impact on the load deflection response of deep beam specimens. Deep beams with higher reinforcement ratio exhibited higher stiffness. Also at the same level of loading displacement increased as the reinforcement ratio increased. Compared to specimen B1, when the ultimate load in the specimen B2, B3, B4 and B5 was increased by 10 %, 18%, 31% and 47% respectively. This resulted in an 11 %, 17%, 52% and 66% respectively.

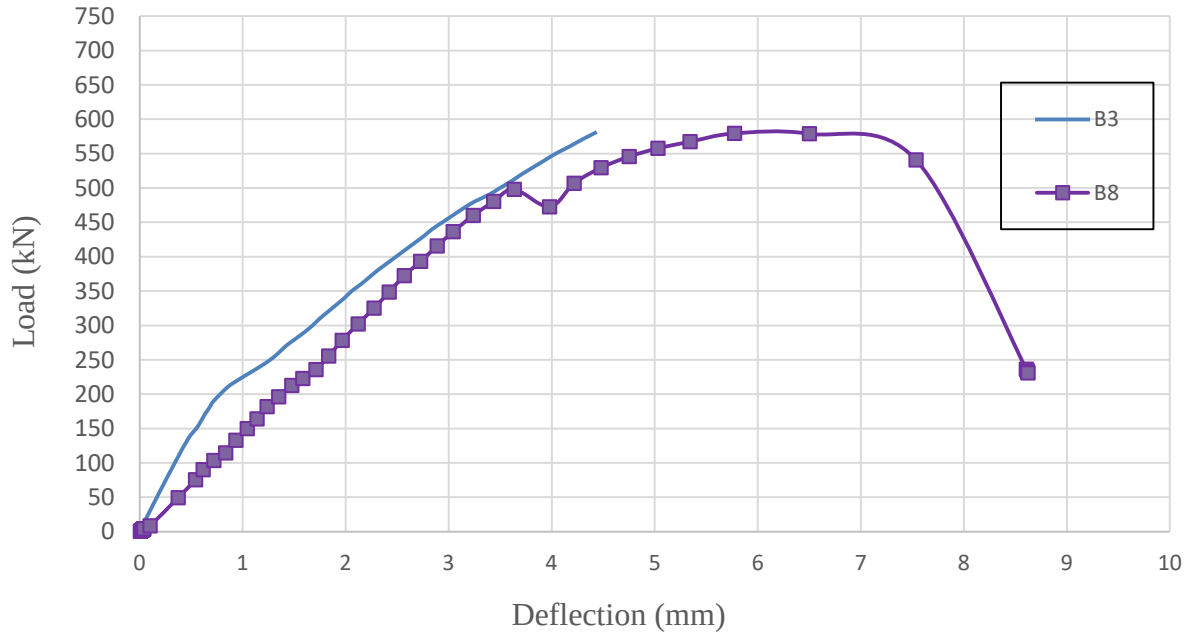

Figure 8. Load deflection relationship for specimens B3 and B8 at failure.

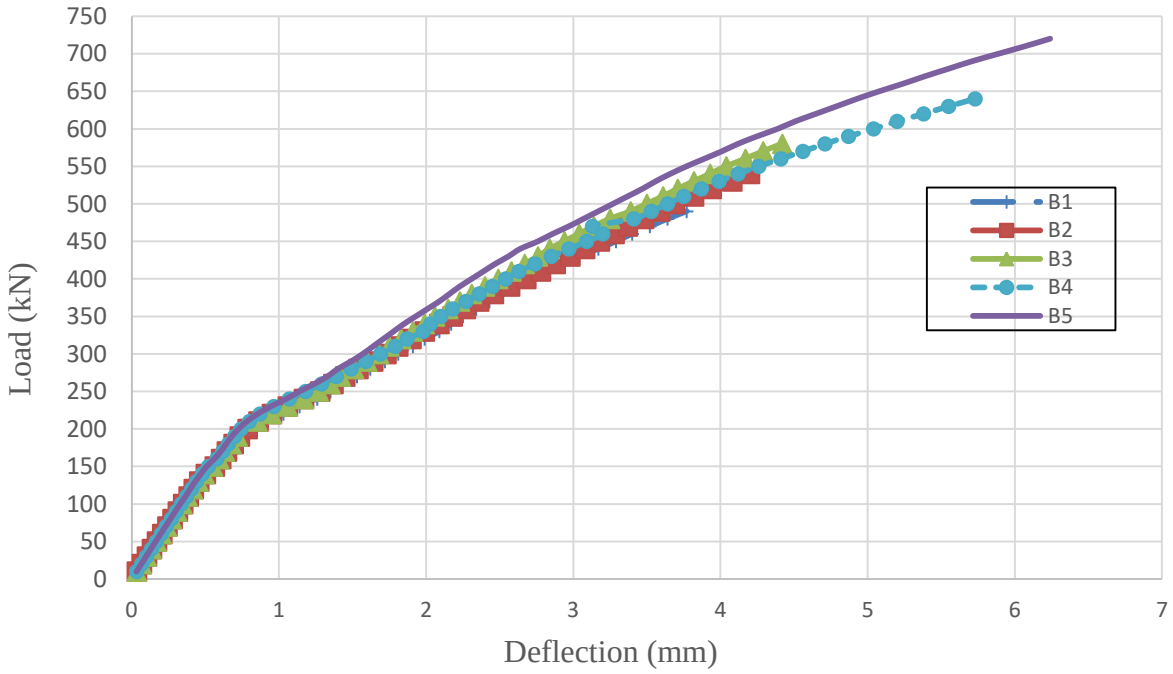

Figure 9 Load deflection relationship for analytical deep beam specimens at failure.

4.3.Ultimate failure load

Table 1 shows the analytical ultimate failure loads and the ACI318-08 predicted values without any safety factor. The ratio of predicted strength to analytical strength varied between 0.58 and 0.73. The ACI provisions' had a conservative prediction more than analytical model.

Table.1 Analytical and predicted ultimate loads

Specimen	Reinforcement ratio (%)	Beam dimension, mm	Analytical failure load, Fa, kN	Predicted failure load, Fp (ACI), kN	Fp/Fa
B1	0.15	200 x 400	500	290	0.58
B2	0.41	200 x 400	540	329	0.61
B3	0.53	200 x 400	580	383	0.66
B4	0.67	200x 400	640	454	0.71
B5	0.79	200 x 400	720	526	0.73

5 .Conclusions

Analytical study of deep beam specimen of reinforcement ratio varied between 0.15% and 0.79% are presented. The following are the most notable findings from these experiments:

Reinforcement ratio exhibited a noticeable effect on the behavior of deep beams; reinforcement ratio should be adopted in deep beams formula as significant factor.

ACI provisions predicted a very conservative ultimate capacity.

6. References

1. ACI Committee 318, "Building Code Requirements for Structural Concrete (ACI 318-05) and Commentary (318R-05)," American Concrete Institute, Farmington Hills, MI, 2005, 430 pp.
2. Moe, J., "Shearing Strength of Reinforced Concrete Slabs and Footings Under Concentrated Loads," Bulletin No. D47, Journal of the Portland cement Association, Research and Development Laboratories, Apr. 1961, 130 pp.
3. Joint ACI-ASCE Committee 326, "Shear and Diagonal Torsion," ACI Structural Journal, V. 85, No. 6, Nov.-Dec. 1988, pp. 675-696.
4. Regan, P. E., and Bræstrup, M. W., "Punching Shear in Reinforced Concrete," Bulletin d'Information No. 168, Comité Euro-International du Béton, Jan. 1985, 232 pp.
5. Regan, P. E., "Symmetric Punching of Reinforced Concrete Slabs," Magazine of Concrete Research, V. 38, No. 136, Sept. 1986, pp. 115-128.
6. Bažant, Z. P., and Cao, Z., "Size Effect in Punching Shear Failure of Slabs," ACI Structural Journal, V. 84, No. 6, Jan.-Feb. 1987, pp. 44-53.
7. Gardner, N. J., "Punching Shear Provisions for Reinforced and Prestressed Concrete Flat Slabs," Canadian Journal of Civil Engineering, V. 23, 1996, pp. 502-510.
8. Sherif, A.G., and Dilger, W. H., "Critical Review of the CSA A23.3-94 Punching Shear Provisions for Interior Columns," Canadian Journal of Civil Engineering, V. 23, No. 5, 1996, pp. 998-1011.
9.